Procedure to determine the impact of the surface film resistance on the hygric properties of composite clay/fibre plasters

McGregor, F, Fabbri, A, Ferreira, J, Simões, T, Morel, J-C & Faria, P

Original citation & hyperlink:
McGregor, F, Fabbri, A, Ferreira, J, Simões, T, Morel, J-C & Faria, P 2017, 'Procedure to determine the impact of the surface film resistance on the hygric properties of composite clay/fibre plasters' *Materials and Structures*, vol 50, no. 4, 193
https://dx.doi.org/10.1617/s11527-017-1061-3

DOI 10.1617/s11527-017-1061-3
ISSN 1359-5997
ESSN 1871-6873

Publisher: Springer

The final publication is available at Springer via http://dx.doi.org/10.1617/s11527-017-1061-3

Procedure to determine the impact of the surface film resistance on the hygric properties of composite clay/fibre plasters

Fionn McGregor*

LGCB-LTDS, UMR 5513 CNRS, ENTPE, Université de Lyon, 69100 Vaulx-en-Velin, France ;

fionn.mcgregor@entpe.fr

Antonin Fabbri

LGCB-LTDS, UMR 5513 CNRS, ENTPE, Université de Lyon, 69100 Vaulx-en-Velin, France ;

antonin.fabbri@entpe.fr

João Ferreira

Dept. of Civil Engineering, NOVA University of Lisbon, 2829-516 Caparica, Portugal

LGCB-LTDS, UMR 5513 CNRS, ENTPE, Université de Lyon, 69100 Vaulx-en-Velin, France ;

jpr.ferreira@campus.fct.unl.pt

Tania Simões

Dept. of Civil Engineering, NOVA University of Lisbon, 2829-516 Caparica, Portugal

LGCB-LTDS, UMR 5513 CNRS, ENTPE, Université de Lyon, 69100 Vaulx-en-Velin, France ;

ts.simoes@campus.fct.unl.pt

Paulina Faria

CERIS and Dept. of Civil Engineering, NOVA University of Lisbon, 2829-516 Caparica, Portugal
paulina.faria@fct.unl.pt

Jean-Claude Morel

Faculty of Engineering, Environment & Computing. Coventry University, UK

ac0969@coventry.ac.uk

**Corresponding author*

Address: LGCB-LTDS, UMR 5513 CNRS, ENTPE, Université de Lyon, 69100 Vaulx-en-Velin, France

Tel: +33(0) 472047744

ABSTRACT

The experimental determination of dynamic mass transfer properties of porous materials such as eco-efficient clay plasters is greatly influenced by the convective conditions at the surface of the material during the test. The measurement of the intrinsic vapour permeability of highly porous materials has shown to present wide discrepancies when the surface film resistance is not known. Therefore, a proper assessment of the hygric properties of clay plasters requires the determination of such resistance to vapour flow. An adapted experimental procedure was used to determine intrinsic water vapour permeability taking into account the influence of the surface film resistance. The moisture buffering test (MBV) was used to measure dynamic exchange behaviour. The results gave evidence on the thickness of the active layer in the material and the impact of surface resistance on the exchange behaviour. A 1D mass transfer model was used to verify the validity of corrected vapour permeability by the surface film resistance and discuss its nature and influence on dynamic results.

Keywords: Surface film resistance, Vapour Permeability, Moisture Buffering, Clay, Biobased, Plasters

Symbol	Description	Units
ρ_d	Dry density	kg/m^3
ϕ	Porosity	(-)

ξ	Moisture capacity	kg/m^3
δ_p	Apparent water vapour permeability	kg/(m.s.Pa)
δ_p^r	Real water vapour permeability	kg/(m.s.Pa)
δ_p^{ISO}	"ISO Correction" water vapour permeability	kg/(m.s.Pa)
δ_a	Water vapour permeability of air	kg/(m.s.Pa)
μ	Water vapour resistance factor	(-)
D_p	Liquid permeability	
p_v^{sat}	Saturation water vapour pressure	Pa
G	Total moisture flow rate	kg/s
A	Area of the specimen	m²
β	Water vapour surface transfer coefficient	kg/(m².s.Pa)
d	Thickness of the material	m
d_a	Thickness of the air layer in the cup	m
u	Water content	kg/kg
w	Water content	kg/m^3
φ	Relative humidity	(-)
Z^s	External surface film resistance	(m².s.Pa)/kg
Z^{Int}	Interior air layer resistance	(m².s.Pa)/kg

1 Introduction

One of the main advantages of raw earth building materials is its hygroscopic behaviour[1–8]. Recent studies have described the hygrothermal models for unconventional building materials and presented some difficulties to model their complex behaviour [9–11]. One of the reasons can be due to imprecise hygric material properties. Further improvement can be brought to the

experimental characterisation of material hygric properties, and, therefore, improving the accuracy of the modelling of the hygrothermal behaviour of hygroscopic building materials [12,13]. A study conducted by Roels et al. [11] realised a round robin test on the measurement of hygric properties of porous building materials. The study concluded on a large variation in results for the water vapour permeability test (dry cup and wet cup). A further recent study investigates the error occurring in the measurement of hygric properties throughout different labs and within the same labs [14] nd the importance of the preconditioning [15].

One reason of these discrepancies on the water vapour permeability test may be caused by the effect of sample thickness, since it changes the ratio of resistance due to the material and the resistance of the surface [16]. The impact of the surface film resistance is usually neglected, because it is assumed to be negligible when compared to the vapour resistance of the material. This assumption may be correct for thick samples with high vapour resistance like concrete. However, recent studies have given estimations of the thickness of the active layer (layer that adsorbs moisture) within the materials and show that a rather thin thickness of the material is active during daily humidity cycles. Padfield [2] had previously estimated the penetration depth through experimental results to be less than 16 mm during a 24h cycle using humidity sensors placed inside of the material. McGregor et al. [8], tested several thicknesses in a Nordtest moisture buffering test on two commercial plasters and compressed earth blocks. The experimentally observed penetration depth for compressed earth blocks was less than 30 mm and less than 12 mm for earth plasters.

It follows that the surface resistance effect may have a significant influence of the hygrothermal behaviour of earthen material and that its effect on both moisture buffering values and permeability tests must be assessed in detail.

To reach this goal, in the present study, samples of three different plaster formulations were prepared at variable thicknesses. The impact of the thickness on the dynamic moisture buffering value test (MBV) test gives experimental indications on the active layer in the material. A method is implemented to measure the surface film resistance during the water vapour permeability test for low vapour resistant unconventional building materials. This method was recently used for low vapour resistant insulation materials like rock wool [16]. The resistance of the surface can then be included in the calculation to determine the true vapour resistance of the material.

Finally, a non-coupled numerical model based on 1D mass conservation under isothermal conditions was solved using Comsol Multiphysics. The model could be compared to the experimental results obtained from the dynamic moisture buffering results, first to validate the corrected values of water vapour permeability and secondly, to investigate the impact of the surface film resistance on the dynamic moisture sorption behaviour.

2 Materials and methods

2.1 Earth plasters formulation

Three earth plaster formulations were studied. These formulations were first selected through a validation of their mechanical performance [17]. The fine fractions of these formulations were:

- **Kaolinite** (F0), a clay with a low specific surface compared to other clays; yet with a high sorption capacity compared to most minerals (particle size: 43% < 2µm and 95% < 80 µm).
- **Ascal 10** (F3) is a fine calcareous-clay material (particle size: 14% < 2 µm and 97% < 80 µm).
- **C mix** (F5) is a commercial formulation based on the ASCAL10 fine calcareous-clay material.

The formulations presented in Table 1 were used to prepare the samples; the mass corresponds to measured values whereas volumes are estimated based on the loose bulk density of the materials.

Each formulation was applied as plasters in a specific framework (50 x 50 cm) [18] at three different thicknesses (1 cm, 2 cm and 4 cm).

Table 1 Plaster composition

		Sand (<2mm)	**Kaolinite**	**Water**	**Straw (30-50 mm)**
F0	Volume (L)	*15.54*	*7.77*	*9.7*	*15.54*
	Mass (kg)	*23.59*	*8*	*9.7*	*0.81*
	% dry mass	*73*	*25*	-	*2.5*
		Sand (<2mm)	**Ascal**	**Water**	**Straw (10-30 mm)**
F3	Volume (L)	*16*	*4*	*8.5*	*15.54*
	Masse (kg)	*24*	*11.06*	*8.5*	*0.78*
	% dry mass	*67*	*31*	-	*2*
		C Mix	**Water**		
F5	Volume (L)	*4*	*2*		

Samples were dried in a controlled environment in a conditioning room at 20±2°C and 60±5% of relative humidity (RH). Periodical measurements were realised to follow the drying stage of the earth plaster samples. Plasters were considered dry when a stable mass was reached.

2.2 Porosity, density and sorption isotherms

After this drying period, each plaster plate was dry cut in four identical parts, the cuts were clean and no visual damage could be observed on the cut samples. Three of them are used for the realisation of the wet cup, dry cup and dynamic tests, while the last one was used to measure the plaster porosity, its dry density, and its sorption-desorption curves.

The samples were first oven-dried at 50°C. The mass of the sample after this stage were considered as dry mass. This temperature was chosen by precaution to avoid any heat degradation of

the organic fibres. The relative humidity within the oven was checked with a portable sensor (Rotronic HygroLog HL-NT), and it was found to be consistently lower than 5% RH.

The apparent dry density is calculated based on the dry mass volume ratio. The porosity is calculated based on standard density values and composition of the plaster. The formulation F0, F3 and F5 had an apparent density of 1596 kg/m^3, 1660 kg/m^3 and 1720 kg/m^3 respectively. The porosities are 33% for the formulation F0 and F3 respectively. The composition of formulation F5 is not known and therefore no porosity could be estimated.

The sorption-desorption isotherms are realized on three representative samples of each formulation (more than 10 g of mass each), following the standard ISO 12571 [19].

The samples were placed in six different RH levels (23, 43, 59, 75, 85 and 97%) and each level was maintained in an isolated box by a corresponding salt solution, the boxes are kept in a controlled conditioning room at 23°C. Two desorption curves were realised. The first one on samples previously equilibrated at 97% and the second one on samples equilibrated at 85% RH. A portable sensor (Rotronic HygroLog HL-NT) was used for a regular control of the RH and the temperature in the boxes.

The samples were weighed periodically (≈ 5 measurements in 5 days) using a scale with an accuracy of 0.01 g. The equilibrium moisture content for each RH level was reached if the change of mass between three consecutive measurements was less than 0.1% of the total mass. Sorption isotherms of these materials were relatively fast to obtain, the mass at each RH level stabilised in a few days.

2.3 Material water vapour resistance

The water vapour permeability was measured according to the standard ISO 12572 [20] using the "wet cup" and the "dry cup" methods. The vapour pressure gradient is created for the wet cup by setting the RH at 60% in the chamber and 85% in the cup, for the dry cup the RH in the cup is set to 23% and in the chamber it remains at 60%. Those levels were chosen for a greater stability of the test conditions. Previous RH measurements in the cup have shown that using silica gel to establish a

hypothetic 0% RH actually yields values drifting from 11 to values close to 17% RH. The RH levels within the cup are maintained using saturated salt solutions as recommended by the ISO 12572 standard. The cup design was done according to the procedure followed by McGregor et al.[7]. A thin bed of silicon was applied in order to seal the samples to the plastic cup. A vapour-tight aluminium tape was used to seal the sides of the sample with the side of the cup. The use of aluminium tape is justified by its properties: it is impermeable and does not adsorb moisture itself [21].

The environmental conditions (60% RH and 23ºC) were constantly controlled by the climatic chamber. Measurements were done periodically, on a scale outside of the chamber, after an initial stabilization period a stable mass flow is reached. For the wet cup test a decrease will be measured while an increase is measured for the dry cup test. A stable mass flow is reached when a linear function between mass variation and time can be established.

2.4 Dynamic moisture exchange behaviour (Moisture Buffering Value)

This test is used to characterize the material's ability to moderate variation of the RH in the indoor environment and it will allow evaluating experimentally the active depth within the material. The moisture buffering test has been performed following the Nordtest protocol [22].

All earth mortar plaster samples were cut to 15 cm x 15 cm squares. Three samples of each thickness (1, 2 and 4 cm) were prepared. The specimens were sealed with aluminium tape in all surfaces except one, in order to have just one exposed surface in contact with the controlled environment. The boundary conditions applied in this test were the use of cycles of 33% RH to 75% RH with time steps of 8 h at high relative humidity and 16 h at low relative humidity.

The mass was measured at set intervals at 0 h, 2 h, 4 h, 6 h, 8 h, 9 h and 24 h for the 24 h cycles, additional measurements were realised at 46 h, 48 h, 50 h, 52 h, 54 h, 70 h, 71 h and 72 h. A scale

with an accuracy of 0.01 g placed outside of the chamber was used to weight the samples. The recording was done outside in order to avoid the vibration created by the ventilation in the climatic chamber and to be able to measure series of samples rather than one sample placed on a scale and recorded continuously. The measurements were realised after a dynamic equilibrium was reach where the variation between the initial and final mass during a cycle do not exceed 5%. This dynamic equilibrium is typically reached after 5 cycles for earthen materials.

2.5 Isothermal 1D mass transfer model

The model used is better described in [23], the mass conservation was formulated to use the relative humidity as the main dependent variable (1D, neglecting the effect of gravity, and considering isothermal evolution):

$$\left(\rho_d \frac{\partial u}{\partial \varphi}\right)\frac{\partial \varphi}{\partial t} = \frac{\partial}{\partial x}\left(\left(\delta_p\, p_v^{sat} - D_p\right)\frac{\partial \varphi}{\partial x}\right) \quad \textbf{(1)}$$

At any time, t, in the sample at 1D position, x, the water content, u, depends on the relative humidity, φ, in the material, which itself depends on the initial boundary conditions, the saturation water vapour pressure, p_v^{sat}, and the vapour, δ_p, and liquid, D_p, permeability.

The following boundary conditions were used (eq. 2a and 2b), when $x = 0$, only the surface film resistance or here expressed by the transfer coefficient, β, determines the value of the relative humidity condition at the surface of the sample linked to the condition of the surrounding environment, RH. Whereas, in the depth of the material, $x = L$, the relative humidity depends on the vapour, δ_p, and liquid, D_p, permeability:

$$\left(\delta_p\, p_v^{sat} - D_p\right)\frac{\partial \varphi}{\partial x} = \beta\, p_v^{sat}(\varphi - RH) \quad \text{at } x = 0 \quad \textbf{(2a)}$$

$$\left(\delta_p\, p_v^{sat} - D_p\right)\frac{\partial \varphi}{\partial x} = 0 \quad at\ x = L \qquad \textbf{(2b)}$$

An important difficulty of the use of eq. (1) is to properly estimated both water vapour permeability, δ_p , and liquid permeability, D_p , as well as their variations with saturation ratio (water volume over total pore volume), which is quite difficult to be experimentally realised at the low saturation degree considered in this study (at 75% of relative humidity, the saturation ratio is lower than 5%) [24]. This is further discussed in section 3.2.3.

The model was numerically solved using the PDE module of COMSOL Multiphysics and where use to simulate the results of the dynamic test (the MBV test).

3 Results

3.1 Sorption isotherms

Figure 1A shows the results of the sorption and desorption from 97%RH. Among all formulations, F0 exhibits a greater moisture adsorption, while the F5 formulation has the lowest. All three materials are poorly hygroscopic when compared to other earth building materials such as compressed earth blocks [8].

The difference between the adsorption and the desorption curves from 97% RH, which is commonly called the hysteresis of moisture content, remains quite limited but is not null (about 10% at 80% RH). This type of curve is referred as type IIb according to Rouquerol et al. [25].

However, to assess the hygroscopic property, realistic hygrometry cycles in buildings commonly do not exceed 85% RH and do not go below 23% RH. The sorption-desorption curves within this range of relative humidity is shown in the Figure 1B. It leads to quite linear relations and almost no

differences between the sorption and the desorption curves. This fact tends to justify the use of a single and constant average moisture capacity ξ, which is defined as the variation of water mass with relative humidity per unit of material volume ($\xi = \rho_d\,(\partial u/\partial HR)$), as a first estimation of the hygroscopic behaviour of the material.

As a consequence of these results, the hysteresis between sorption and desorption curves is neglected in the following of this paper and only the adsorption curve will be used for modelling purposes.

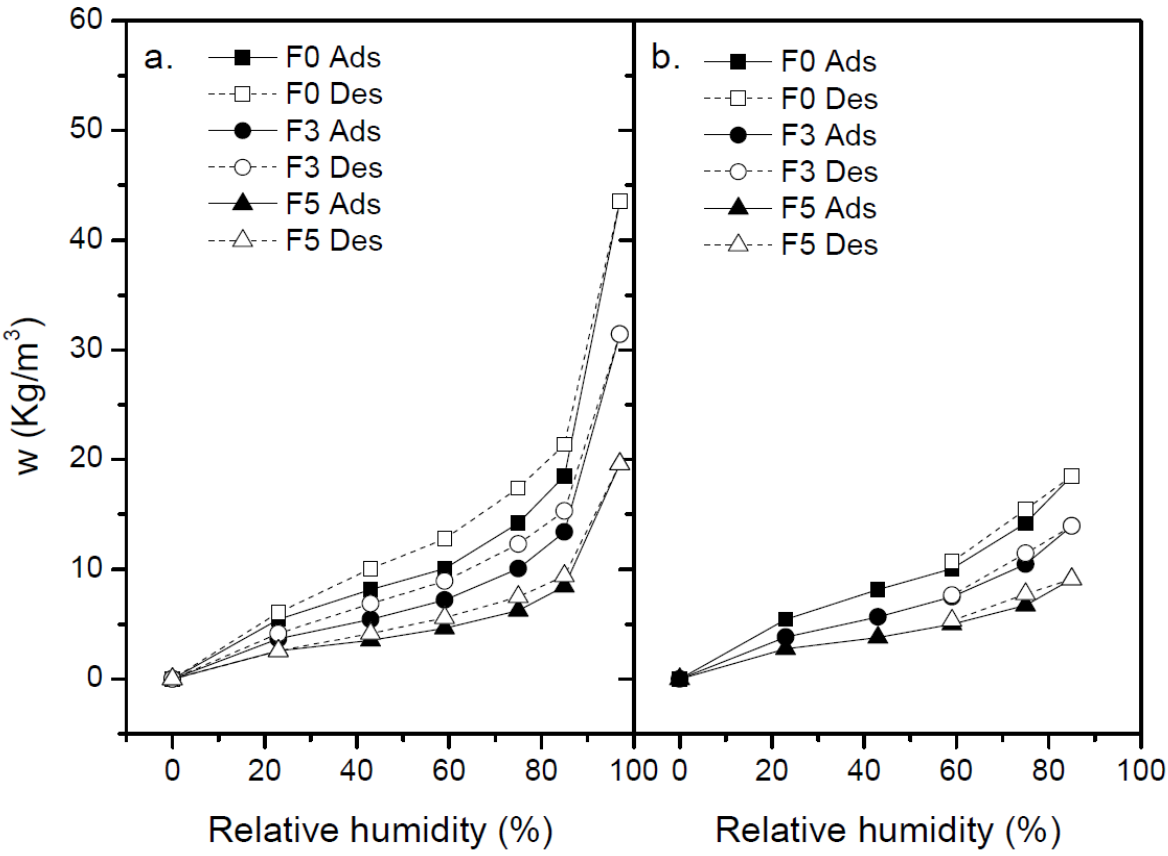

Figure 1 Sorption isotherms and desorption from 97% RH (a.) and 85% RH (b.)

3.2 Water vapour permeability

3.2.1 Water vapour permeability Standard analysis

At first, the water vapour permeability is obtained using the standard EN ISO 12572 [20] for each thickness of every material. From the experimental mass variation of the cup assembly (wet or dry) a regression line $G = \Delta m/\Delta t$ (kg/s) is determined when the permanent state is reached. The water vapour permeability is then expressed using Fick's law of diffusion by (eq.3):

$$\delta_p = \frac{G \cdot d}{\mathrm{A} \cdot \Delta p_v} \quad \textbf{(3)}$$

where A (m^2) is the exposed surface of specimen, *d* is the thickness of the sample and Δp_v (Pa) is the water vapour pressure difference across the sample.

The vapour resistance factor is often used rather than the water vapour permeability. The vapour resistance factor, μ, is the ratio between the water vapour permeability of air (δ_a) and of the material (δ_p) (eq. 4):

$$\mu = \frac{\delta_a}{\delta_p} \quad \textbf{(4)}$$

The value of δ_a can be estimated from the relation given In Künzel [26] (eq. 5):

$$\delta_a \approx 2 \times 10^{-7} \frac{T^{0.81}}{p_0} \ [\mathrm{kg/(m\ s\ Pa)}] \quad \textbf{(5)}$$

Where T is the ambient air temperature (K) and p_0 is its pressure (Pa). Thus, at 23°C and at average atmospheric pressure (101325 Pa), δ_a=1.97 10^{-10} kg/(m s Pa).

The water vapour resistance factor obtained when no correction is made on the experimental results to include the effect of the surface resistance, "No correction", is given in Figure 2.

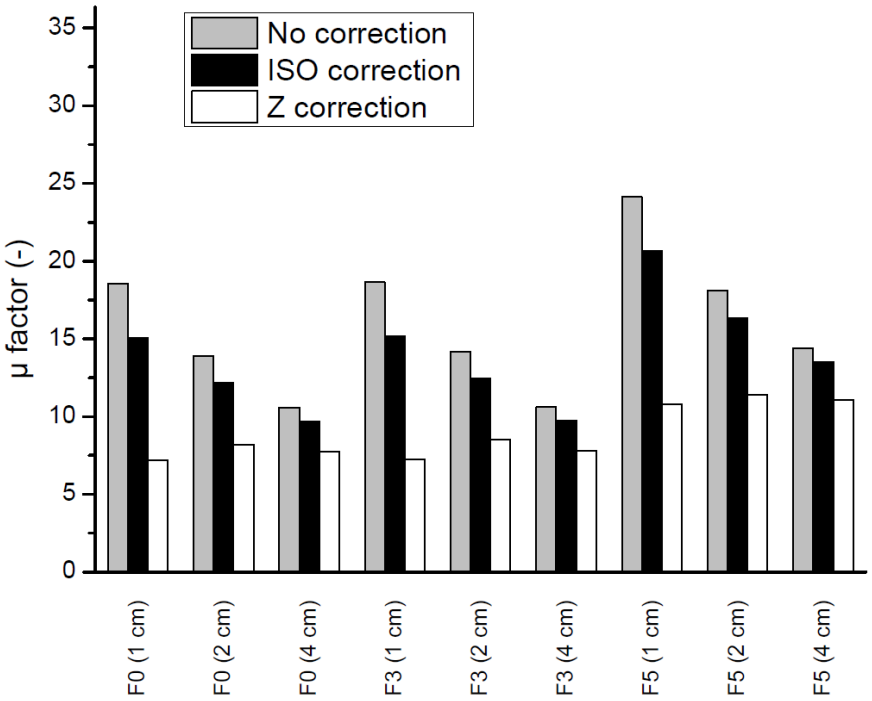

Figure 2 Calculated values of μ factor with and without corrections

The correction that is given in the EN ISO 12572 [20] is to include the resistance to water vapour diffusion presented by the air layer between the sample and the salt solution. This correction is normally recommended when the water vapour diffusion-equivalent air layer thickness ($s_d = \mu \cdot d$) is lower than 0.2 m. It assumes that the transport of vapour within the cup is only made by diffusion (no convection) and it leads to the equation 6, where d_a is the thickness of the air layer between the salt solution and the sample. It will be referred to as the "ISO correction":

$$\delta_p^{ISO} = \frac{G \cdot d}{A \cdot \Delta P_V - G \frac{d_a}{\delta_a}} \quad ; \quad \mu^{ISO} = \frac{\delta_a}{\delta_p^{ISO}} \tag{6}$$

The calculated water vapour permeability of the air at $\delta_a = 1.97\ 10^{-10}\ \mathrm{kg/(m\ s\ Pa)}$ and the thickness of the air layer is d_a=30 mm at 23°C are reported in Figure 2 as "ISO correction". From the values in Figure 2 it can be noticed that there is a significant difference of measured μ factor for a

same material at different thicknesses for the values with no correction and the ISO correction. The preparation method of all thickness plasters was scrupulously the same. Therefore, no apparent heterogeneities can explain such differences and the effect of the surface film resistance are considered as the cause. A further correction can be applied to take into account the effect of an immobile air layer at the very close external surface of the material.

3.2.2 Correction with surface film resistance

To obtain the real vapour permeability of the material whatever the thickness using the method of the cup test, the effect of the surface film resistance at the external surface of the sample must also be taken into account, in the cup and outside the cup. Experimentally, the value of the surface film resistance depends among others on the texture of the material surface and air velocity in the chamber.

However, only a global surface film resistance, Z, can be estimated from the experimental results. A method was recently used by Vololonirina et al. [16,27] to experimentally determine the surface film resistance. At least three different thicknesses of the material need to be measured to plot a relation between thickness of material and the apparent resistance of the material, the following limit (eq.7) when the thickness of the material tends to zero gives the global surface resistance

$$\lim_{d\to 0}\left(d\frac{1}{\delta_p} = d\frac{1}{\delta_p^r} + Z\right) = Z \qquad \textbf{(7)}$$

where δ_p^r is the real water vapour permeability, while δ_p is the apparent water vapour permeability which is calculated through the relation (3).

The intercept of the linear relation gives the values of the global surface resistance,Z. The values obtained for the F0 and F3 samples are 6.10^8 (m².s.Pa)/kg and 7.10^8 (m².s.Pa)/kg for the F5 sample. The calculate water vapour resistance including the external surface film resistance will be referred to as the "Z correction", the values are given in Figure 2. It can be noticed that the values are more consistent whatever the thickness of the material.

3.2.3 Impact of the water saturation level on the cup test

It is well known in unsaturated soil mechanics that both liquid and gaseous phases fill the open porosity. Greater saturation level reduces the amount of porosity available for water vapour diffusion but in turn increases the liquid permeability.

Therefore, the impact of the liquid mass transfer due to a higher saturation level on the experimental test which aim at quantifying diffusion should be properly evaluated.

The sorption isotherms of the material presented in section 3.1 show that the saturation level relative variation remains lower than 5% for all the tested plasters when the relative humidity varies from 33% to 75%. It can be assumed that for such a low saturation level both vapour and liquid permeability remain constant during the hygric test conducted in this study and that the liquid transport is negligible. and that the measured apparent value of δ_p is sufficient to estimate properly ($\delta_p\ p_v^{sat} - D_p$).

An experimental validation of this assumption can be made by comparing dry cup and the wet cup test results. In Figure 3, the water resistance factor of plasters obtained by the wet cup test is compared to the values obtained by the dry cup test. The results for F0 and F3 formulations do not show significant difference, suggesting that the variation of the saturation from dry cup to wet cup is negligible and does not affect considerably the mass transfer. The F5 formulation shows on the opposite a significant difference between the dry cup and wet cup results. The diffusion of water

vapour for the F5 formulation is more impacted by the saturation level of the pore network than the F0 and F3 formulations. Therefore, this assumption is only valid for formulations F0 and F3. In consequence, only the F0 formulations is chosen for numerical validation of the impact of the surface film resistance and diffusion is considered as the only mass transfer process, the liquid permeability, D_p, in the mass transfer model (eq. 1) will be neglected.

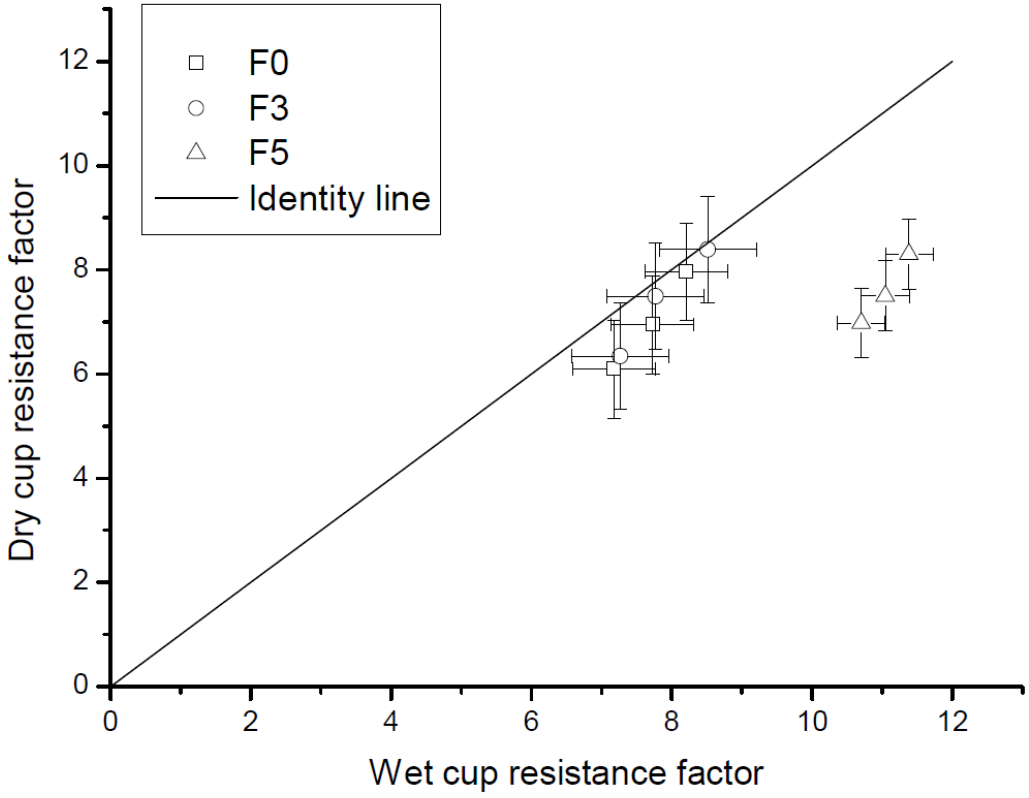

Figure 3 Comparison between wet cup and dry cup results

3.3 Results of dynamic tests for cycles of 24 hours and 72 hours

The dynamic moisture exchange capability of the samples is estimated using the MBV test described previously and considering two cycles. In Figure 4, the results of the moisture uptake and release during the 24 h-cycles are shown for samples F0, F3 and F5. Each plaster formulation was tested at different thicknesses. It can be noticed that, for F0 and F3 formulations, no significant difference between the thicknesses can be observed. This leads to conclude that the penetration depth of moisture into the bulk of the sample during an 8 h phase of high humidity load remains below 1 cm for F0 and F3 plaster formulations. The results obtained for the F5 formulation show greater adsorbed moisture content for the 2 cm and 4 cm thick samples. In consequence this suggests that the 1 cm thick samples are approaching equilibrium during this phase.

It is worth to mention here that the moisture adsorption of all three formulations gives satisfactory results regarding buffering potential. The Nordtest classifies materials with adsorption capacity over 42 g/m² as good buffering materials [22]. Therefore F0 and F3 formulations are good buffering materials just above this limit whereas the F5 formulation would have to be at least 2 or 4 cm thick to reach this level. This performance is however relatively low when compared to values from previous publications [7,8,23].

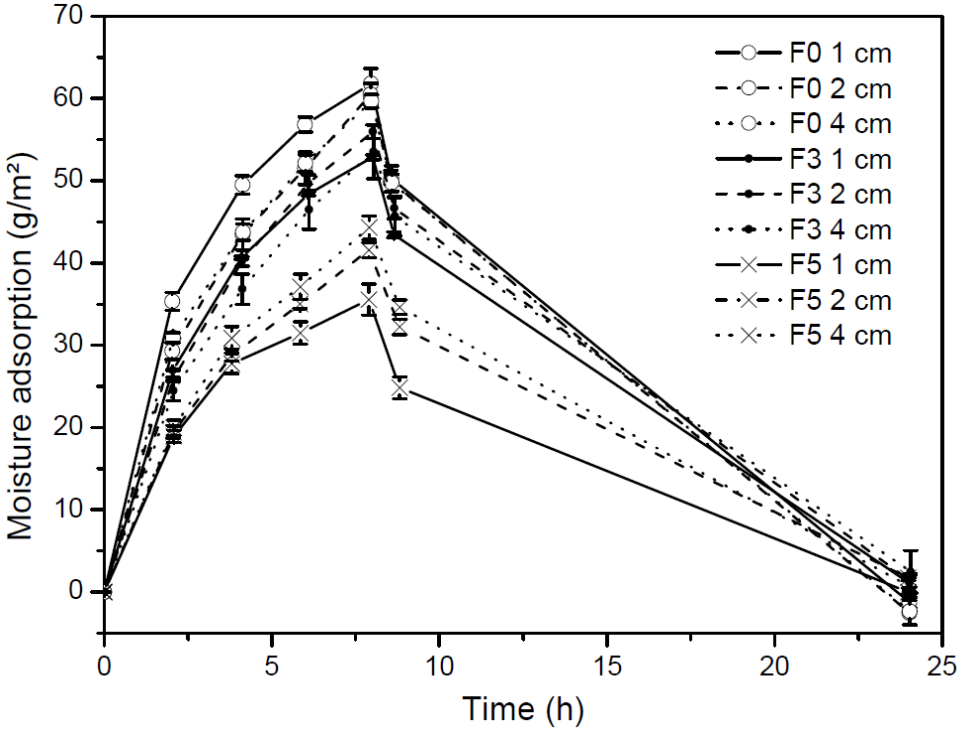

Figure 4 Results of the MBV test for 24 h cycles

The results of the moisture buffering test with time cycles of 24 h at 75% RH and 48 h at 33% RH are shown in Figures 5. Due to the impossibility to weight the samples during night time, a considerable gap is left in the 24 h adsorption phase between the measure at 6 h and 21 h. It is however possible to see the difference in adsorption between the different thicknesses.

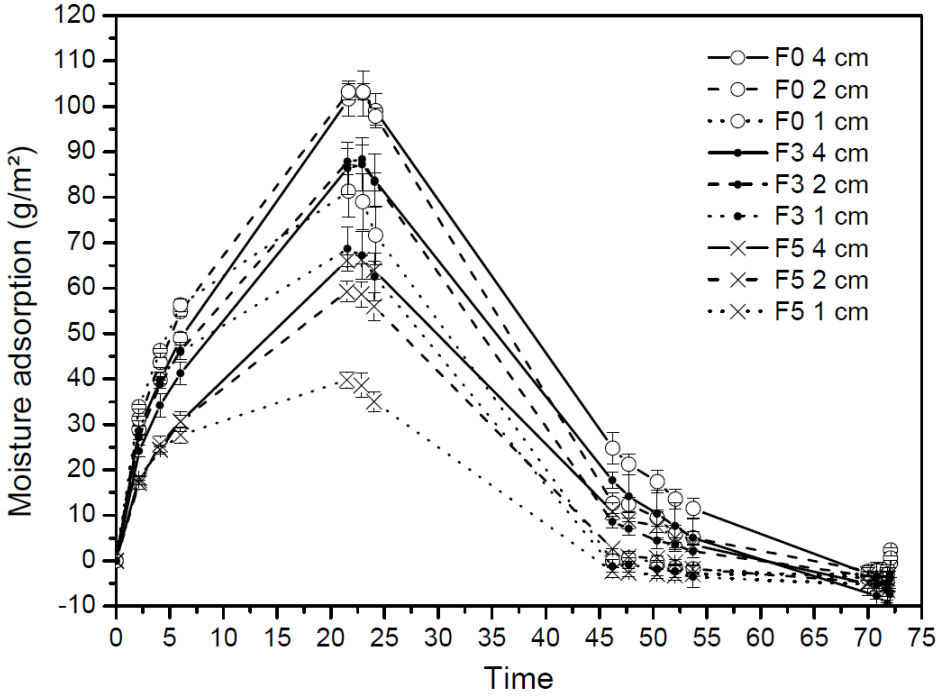

Figure 5 Results of the MBV test for 72 h cycles

For all formulations, the 1 cm thick samples are reaching lower maximal adsorbed moisture content. For the formulations F0 and F3 the adsorbed moisture for the 2 cm thick samples remains the same than for the 4 cm thick samples. The penetration depth is therefore between 1 and 2 cm. Only for the formulation F5 it can be observed that the 2 cm thick samples also reach lower values than the 4 cm thick samples which indicate that the penetration depth for the formulation F5 is between 2 and 4 cm.

4 Discussion

4.1 Validation of the corrected water vapour resistance factor

To validate the corrected value of the water vapour permeability a simulation of the dynamic results was done by solving the differential equation described in section 2.5. The numerical simulation was done for the F0 sample at 4cm and with a vapour resistance factor of 12.3 and 7.55. The usually recommended value of 2.10^{-8} kg/(m².s.Pa) is used as the external surface transfer coefficient in the MBV test which corresponds to a surface film resistance of 5.10^{7} (m².s.Pa) / kg [28]. The results of the simulation using the ISO correction water vapour resistance (µISO) are shown in Figure 6. The simulation shows an under estimation of the moisture buffering results indicating an overestimated water vapour resistance of the material.

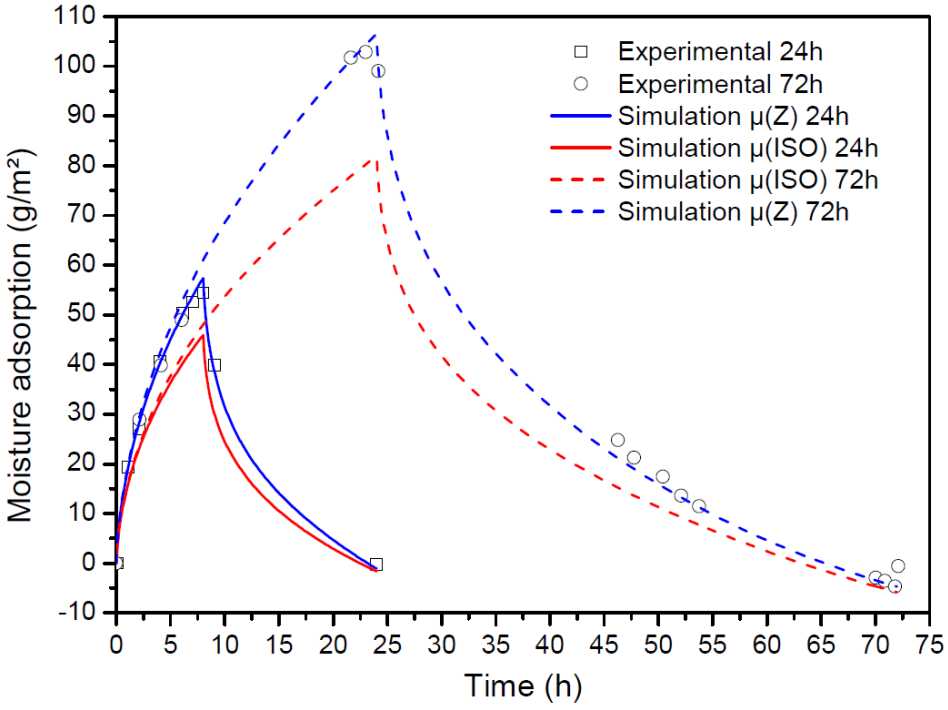

Figure 6 Simulation with the ISO and Z corrected water vapour permeability

The simulation using the corrected vapour resistance factor by the external surface resistance is also shown in Figure 6. The simulation gives consistent results with the experimental

data for both 24h and 72h. Based on this numerical simulation it can be concluded at first that a correction of the water vapour permeability using the Z correction is valid.

4.2 Analysis of the surface film resistance

In thermal analysis, a heat convection coefficient is used to express the convective exchange of heat over a defined surface. The inverse gives the thermal surface resistance. This resistance of a surface over which convective exchanges occur can be explained by the fact that air velocity reaches zero at the contact of the material. Analogy can be made with the mass transfer coefficient and the surface film resistance. Any transfer can be expressed by the equivalent transfer coefficient, in this study named, β, or by the resistance, Z. This coefficient depends on many different parameters and can only be experimentally determined.

The method described used in this study relies on the experimental determination of global surface resistance during the cup test. This global coefficient can however be further described, because it is essentially composed of the resistance of the air layer in the cup, the resistance of the surface in the cup and the resistance of the external material surface. In Figure 7, the setup of the wet cup design is schematically represented, the β_1 and β_2 coefficients represent the surface film resistance at the interior surface and the external surface respectively. The first approximation made is that the internal surface film resistance is negligible as there is no forced convection in the cup, so the total internal resistance can be expressed by the resistance due to the thickness of the air layer within the cup.

Therefore, the total internal resistance in the cup to the diffusion of water vapour, Z_{int}, can be expressed by (eq. 8) :

$$Z_{int} = \frac{d_a}{\delta_a} \tag{8}$$

This needs to be clarified, the known vapour pressure is at the surface of the saturated salt solution expressed by P_{v1} in Figure 7 and the measured vapour pressure in the chamber is expressed by P_{v2}. The real vapour pressure at the surface of the material, P_{v1}^* and P_{v2}^*, is affected by the resistance of the air layer and the resistance of the surface film resistance.

The corrected vapour pressure at the surface of the material (ΔP_v^*) is obtained in equation 9a and 9b where $\Delta P_{v1} = (P_{v1} - P_{v1}^*)$ and $\Delta P_{v2} = (P_{v2} - P_{v2}^*)$:

$$\Delta P_v^* = \Delta P_v - \Delta P_{v1} - \Delta P_{v2} \tag{9a}$$

$$\Delta P_v^* = \Delta P_v - \frac{G}{A \times \frac{\delta_a}{d_a}} - \frac{G}{A \times \beta_2} \tag{9b}$$

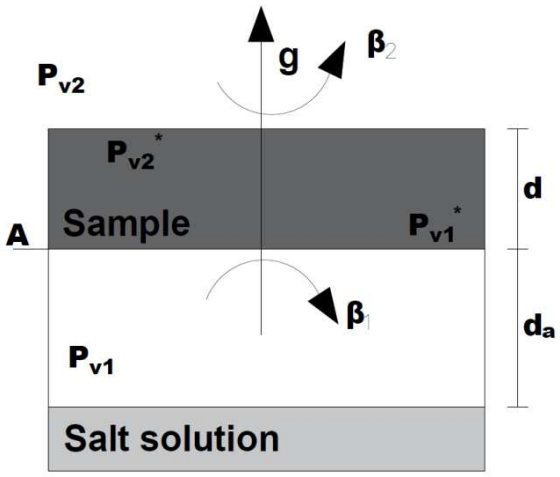

Figure 7 Layout of the process during the test

The value of the transfer coefficient due to the external film resistance can be calculated as the interal resitance Z_{int} is given by the thickness of the air and the vapour permeability of the air, both known parameters.

The surface film resistance is therefore expressed by equation 10:

$$Z^s = \frac{1}{\beta_2} = Z - \frac{d_a}{\delta_a} \quad (10)$$

This leads to discuss on the values of the external surface film resistance obtained from this relation. The values are presented in table 2, where Z^s is surface film resistance of the external surface during the wet cup test. For samples F0 and F3, the results are consistent a part for the dry cup test of the F0 sample, and present a value of about 4.10^8 (m².s.Pa)/kg. This value is about a factor 10 higher than the usually recommended value for building materials surface film resistance of 5.10^7 (m².s.Pa)/kg. It is comparable with some values found in the literature for polyurethane foams.

Table 2 External surface film resistance and associated transfer coefficient from this study and from literature

Reference		Z^s (m².s.Pa/kg)	β_2 (kg/m².s.Pa)
Results plaster F0	wet cup	$3.96.10^8$	$2.42.10^{-9}$
	dry cup	$1.89.10^8$	$5.29.10^{-9}$
Results plaster F3	wet cup	$4.12.10^8$	$2.42.10^{-9}$
	dry cup	$3.66.10^8$	$2.73.10^{-9}$
Results plaster F5	wet cup	$5.05.10^8$	$1.98.10^{-9}$
	dry cup	$5.57.10^8$	$1.80.10^{-9}$
Plaster F0 MBV test		$6.53.10^7$	$1.53.10^{-8}$
[29] Water surface		2.10^7	40.10^{-8}-5.10^{-8}
[30] Paper surface		4.3-$5.4.10^7$	$2.3.10^{-8}$-$1.8.10^{-8}$
[16] Rock wool surface		$4.3.10^7$-2.10^8	5.10^{-9}-$2.3.10^{-8}$

[16] Polyurethane foam	$1.9.10^{8}$-$6.9.10^{8}$	$5.4.10^{-9}$-$1.46.10^{-9}$
[31] Earth masonry	$1.25.10^{7}$-$9.6.10^{6}$	$7.95.10^{-8}$-$10.43.10^{-8}$

In this study, two different climatic chambers are used, one for the water vapour permeability test (chamber A: the cup test), and another one for the moisture buffering test (chamber B : MBV test). The ventilation in chamber A is lower then in the chamber B mainly due to the type of test running, during the water vapour permeability test the chamber is set to a constant RH whereas during the MBV test the chamber is running daily cycles therefore necessating more ventilation to adjust the values. However, in both chambers the average air velocity is over the recommended 0.1 m/s.

As it is showed in the previous section, the simulation of the dynamic moisture exchange using the recommended value for the external surface film resistance of 5.10^7 (m².s.Pa)/kg ($\beta = 2.10^{-8}$) gives satisfactory results for the conditions in the climatic chamber B, see Figure 8 for 24h cycles and Figure 9 for 72h cycles. On the opposite, when the calculations are made with the value of the surface film resistance experimentally determined from the wet cup tests (namely Z^s), the dynamic behaviour is largely underestimated. What's more, this value of surface film resistance has been compared to the one experimentally determined by measuring the mass variation over time of a water cup in the two climatic chambers. Such method of the water cup was previously described in the literature by [31]. This method allows determining the transfer coefficients in other conditions for earth plasters by using the water cup as a neutral indicator of the conditions in each chamber. It leads to respective values of Z_{0A} =2.3 10^7 (m².s.Pa)/kg for the climatic chamber A and Z_{0B} =2.2 10^7 (m².s.Pa)/kg for the climatic chamber B, which are both significantly lower than the measured values of Z^s.

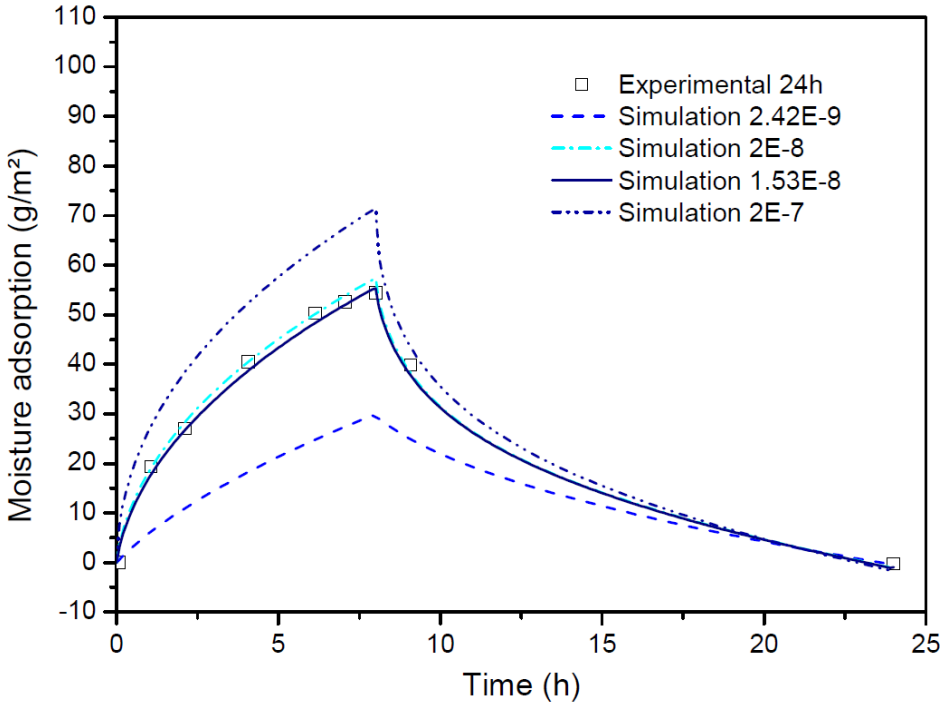

Figure 8 Simulation for the impact of surface film resistance at 24h

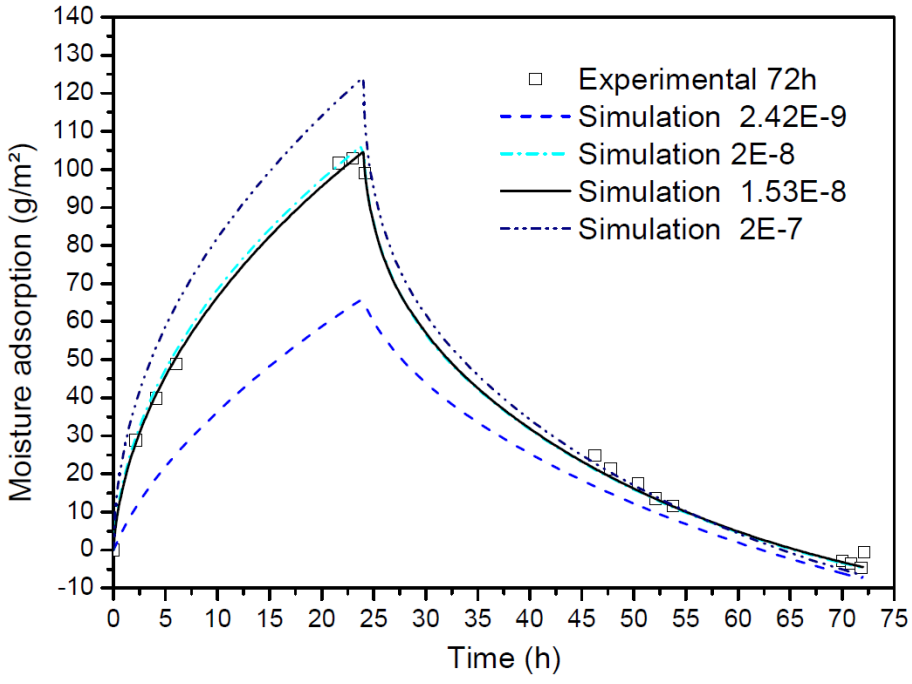

Figure 9 Simulation for the impact of surface film resistance at 72h

Actually, to find some consistencies between the surface film resistances of the water cups and the samples in the both conditions (condition A for the wet cup test, and condition B for the MBV test), it is proposed to use the transfer coefficients (inverse of resistance) with a corrective non-dimensional factor, see Figure 10, which will be named at first the surface correlation factor and denoted by α so that:

$$\beta_A = \alpha \left(\frac{1}{\beta_{0A}} + \frac{d_a}{\delta_a} \right)^{-1} \quad \textbf{(11)}$$

$$\beta_B = \alpha \beta_{0B} \quad \textbf{(12)}$$

Where β_A and β_B are the global moisture exchange coefficient at the surfaces of the porous material for respectively the cup test (both surfaces and air layer) and the MBV test (only the non-wrapped surface), while $\beta_{0A} = 1/Z_{0A}$ and $\beta_{0B} = 1/Z_{0B}$ are the moisture exchange coefficient for a pure water surface at the same external conditions. Therefore, α is the coefficient between the exchange over a surface of pure water and the material surfaces in the same conditions. It is assumed that α remains constant in both chambers as it should only be influenced by the

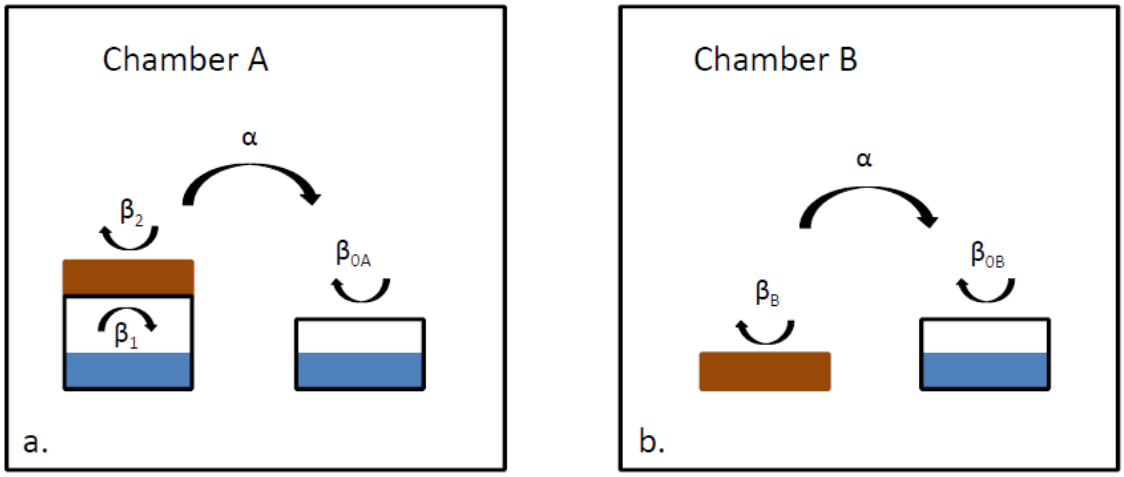

Figure 10 Relative mass transfer coefficient for different experimental conditions

difference of surface of the material (water or earth plaster). Also the cups should be positioned close to each other to have the same convective conditions. The global transfer coefficient for the material in chamber A (represented by $\beta_1 + \beta_2$ in the Figure 10) is β_A =1.7x10^{-9} kg/(m^2.s.Pa) whereas the measured mass transfer coefficient of the water cup is β_{0A}=4.3x10^{-8} kg/(m^2.s.Pa), therefore the equation 11 gives $\alpha \approx 0.34$. The measured value of β_{0B} is 4.5x10^{-8} kg/(m^2.s.Pa) in chamber B and therefore β_B is estimated by $\alpha\beta_{0B}$=1.5x10^{-8} kg/(m^2.s.Pa). When comparing directly the external exchange coeffcients rather than taking a global coefficient in chamber, then α becomes extremely low and the values of β_B in chamber becomes too low. This suggest that the estimation of β_1 only by the resistance due to the thickness of the air layer may not be correct and that it leads to an

overestimation of the external surface film resistance. The values found for β_2 are too low. This observation is consistent when comparing the values of the external surface film resistance with literature values in table 2. Furthermore, such values would correspond to unrealistic values of the equivalent resistance of air layer around 8 cm thick. At this stage only the global resistance measured during the cup test can be used as a reliable value.

In Figures 8 and 9, the simulation obatined using the different external transfer coefficients are compared. The external transfer coefficient obtained directly from the cup test by the determination of the global surface resitance is too low and can be discarded to use as such for the dynamic test. The calculated value from the water cup results is close to the recommended value and both show very similar results. When further increasing the external transfer coefficient to $2x10^{-7}$ the adsorption of moisture is increased. This indicates that the surface film resistance is still a limiting factor for moisture adsorption even with strong air velocities (forced convection in the chamber) used during the test. A similar conclusion on the impact of the surface film resistance can be found in the literature [33] on other building materials.

5 Conclusion

Three formulations of earth mortar plasters were tested regarding their hygric properties. The water vapour permeability, the sorption isotherms and their dynamic response to a cycle representing a typical daily humidity load were tested. The plaster samples were prepared and tested with three different thicknesses, 1 cm, 2 cm and 4 cm, the penetration depth could be determined, in other words, the thickness of the layer that is active within the material during daily humidity variations.

The experimental results indicate a penetration depth below 2 cm for all formulations and below 1 cm for two formulations during 24 h cycles. Further measurements were realized with 72h cycles. The 72h cycle results show a lower moisture adsorption for the samples with a thickness of 1 cm indicating that the penetration depth lies between 1 and 2 cm.

The results of the cup test showed an influence of the thickness of the samples on the results. It could be concluded that the thinner the samples the more they were affected by the surface film resistance. Therefore, a global surface resistance was determined based on the measure of several plaster thicknesses by the cup test. A numerical simulation of the dynamic results from the MBV test validated the use of the corrected water vapour resistance which included the global surface resistance.

The simulation could then be used to investigate the impact and the nature of the surface film resistance. At first the, the simulation results have shown that the external surface film resistance deduced from the global surface resistance obtained during the cup test is not valid. This leads to question the validity of the hypothesis which assumes the resistance in the cup to be correctly estimated by the resistance to diffusion of the air thickness between the salt solution and the material. A method using the evaporation rate of pure water placed in equivalent conditions gave consistency between the global surface resistance during the cup test and the external surface film resistance during the dynamic test.

For both hygric tests, there is evidence that they are strongly impacted by the surface film resistance, unfortunately those are frequently considered as negligible in the literature. An analysis of the surface film resistance should always be included when measuring hygric parameters of biobased and raw earth buildings materials. At this stage the use of a global surface film resistance to estimate the water vapour resistance is validated. The determination of the external resistance

based on the global resistance could not be validated and needs further inquiries into the relative origin of the global resistance (internal, external).

The physical nature of this surface film resistance should be further investigated also through a precise characterisation of surface roughness and its impact on an immobile boundary layer.

Acknoledgements

The research leading to these results has received funding from the People Programme (Marie Curie Actions) of the European Union's Seventh Framework Programme (FP7/2007-2013) under REA grant agreement n. PCOFUND-GA-2013-609102, through the PRESTIGE programme coordinated by Campus France. The authors wish to thank the French National Research Agency – France (ANR) for funding project BIOTERRA – ANR – 13 – VBDU – 0005 Villes et Bâtiments Durables.

Compliance with ethical standards

Conflict of interest: The authors declare that they have no conflict of interest

References

[1] B. Eshoj, T. Padfield, The use of porous building materials to provide a stable relative humidity, in: Preprints of the ICOM-CC Conference, James and James, 1993: pp. 605–609.

[2] T. Padfield, The role of absorbent building materials in moderating changes of relative humidity, PhD Thesis, The Technical University of Denmark, 1998.

[3] M. Hall, D. Allinson, Analysis of the hygrothermal functional properties of stabilised rammed

earth materials, Building and Environment. 44 (2009) 1935–1942.

[4] D. Allinson, M. Hall, Humidity buffering using stabilised rammed earth materials, Construction Materials Proceedings of the Institution of Civil Engineers. 165 (2012) 335–344.

[5] G. Minke, Building With Earth: Design and Technology of a Sustainable Architecture, Birkhäuser Architecture, Basel, Switzerland, 2012.

[6] P. Melià, G. Ruggieri, S. Sabbadini, G. Dotelli, Environmental impacts of natural and conventional building materials: A case study on earth plasters, Journal of Cleaner Production. 80 (2014) 179–186. doi:10.1016/j.jclepro.2014.05.073.

[7] F. McGregor, A. Heath, E. Fodde, A. Shea, Conditions affecting the moisture buffering measurement performed on compressed earth blocks, Building and Environmenti. 75 (n.d.) 11–18.

[8] F. McGregor, A. Heath, A. Shea, M. Lawrence, Moisture buffering capacity of unfired clay masonry, Building and Environment. 82 (n.d.) 599–607.

[9] S. Yu, M. Bomberg, X. Zhang, Integrated methodology for evaluation of energy performance of the building enclosures: Part 4 - material characterization for input to hygrothermal models, Journal of Building Physics. 35 (2012) 194–212. doi:10.1177/1744259111420071.

[10] S. Yu, M. Bomberg, X. Zhang, Integrated methodology for evaluation of energy performance of the building enclosures: Part 5-Application of the proposed hygrothermal characterization, Journal of Building Physics. 36 (2012) 178–197. doi:10.1177/1744259111420071.

[11] S. Roels, J. Carmeliet, H. Hens, O. Adan, H. Brocken, R. Cerny, Z. Pavlik, C. Hall, K. Kumaran, L. Pel, Interlaboratory comparison of hygric properties of porous building materials, Journal of Thermal Envelope and Building Science. 27 (2004) 307–325.

[12] M. Woloszyn, A.-C. Grillet, L. Soudani, J. Morel, A. Fabbri, Potential of existing whole-building

simulation tools to assess hygrothermal performance of rammed earth construction, in: D. Ciancio, C. Beckett (Eds.), Rammed Earth Construction: Cutting-Edge Research on Traditional and Modern Rammed Earth, CRC Press, Perth, 2015: p. 185.

[13] L. Soudani, A. Fabbri, J.-C. Morel, M. Woloszyn, P.-A. Chabriac, Assessment of the validity of some common assumptions in hygrothermal modelling of earth based materials, Energy and Buildings. 16 (2016) 498–511.

[14] C. Feng, H. Janssen, Y. Feng, Q. Meng, Hygric properties of porous building materials: Analysis of measurement repeatability and reproducibility, Building and Environment. 85 (2015) 160–172. doi:10.1016/j.buildenv.2014.11.036.

[15] C. Feng, Q. Meng, Y. Feng, H. Janssen, Influence of Pre-conditioning Methods on the Cup Test Results, Energy Procedia. 78 (2015) 1383–1388. doi:10.1016/j.egypro.2015.11.158.

[16] O. Vololonirina, B. Perrin, Inquiries into the measurement of vapour permeability of permeable materials, Construction and Building Materials. 102 (2016) 338–348. doi:10.1016/j.conbuildmat.2015.10.126.

[17] F. Rojat, M. Olivier, A. Mesbah, B. Xiao, Mechanical Characterization of Natural Fibre-Reinforced Earth Plasters, in: ICBBM 2015 - First International Conference on Bio-Based Building Materials, At Clermont-Ferrand, France, 2015: pp. 64–71.

[18] E. Hamard, J.-C. Morel, F. Salgado, A. Marcom, N. Meunier, A procedure to assess the suitability of plaster to protect vernacular earthen architecture, Journal of Cultural Heritage. 14 (2013) 109–115. doi:10.1016/j.culher.2012.04.005.

[19] ISO-12571, Hygrothermal performance of building materials and products.Determination of hygroscopic sorption properties, (2000).

[20] ISO-12572, Determination of water vapour transmission properties, (2001).

[21] K. Svennberg, Moisture buffering in the indoor environment, PhD Thesis, Building Physics, LTH, Lund University, 2006.

[22] C. Rode, R.H. Peuhkuri, L.H. Mortensen, K.K. Hansen, B. Time, A. Gustavsen, T. Ojanen, J. Ahonen, K. Svennberg, J. Arfvidsson, Moisture buffering of building materials, BYG·DTU R-126, Department of Civil Engineering, Technical University of Denmark, 2005.

[23] S. Dubois, F. McGregor, A. Evrard, A. Heath, F. Lebeau, An inverse modelling approach to estimate the hygric parameters of clay-based masonry during a Moisture Buffer Value test, Building and Environment. 81 (2014) 192–203.

[24] F. Osselin, A. Fabbri, T. Fen-Chong, J.M. Pereira, A. Lassin, P. Dangla, Experimental investigation of the influence of supercritical state on the relative permeability of Vosges sandstone, Comptes Rendus - Mecanique. 343 (2015) 495–502. doi:10.1016/j.crme.2015.06.009.

[25] F. Rouquerol, J. Rouquerol, K.S.W. Sing, Adsorption by Powders and Porous Solids: Principles, Methodology and Applications, Academic Press, 1999.

[26] H.M. Künzel, Simultaneous heat and moisture transport in building components, One-and two-dimensional calculation using simple parameters. IRB-Verlag Stuttgart 1995.

[27] O. Vololonirina, M. Coutand, B. Perrin, Characterization of hygrothermal properties of wood-based products – Impact of moisture content and temperature, Construction and Building Materials. 63 (2014) 223–233. doi:10.1016/j.conbuildmat.2014.04.014.

[28] H. Kunzel, Simultaneous Heat and Moisture Transport in Building Components, One-and two-dimensional calculation using simple parameters. IRB-Verlag Stuttgart 1995.

[29] L. Wadsö, Surface mass transfer coefficients for wood, Drying Technology. 11 (1993) 1227–1249.

[30] L.H. Mortensen, R. Peuhkuri, C. Rode, Full scale tests of moisture buffer capacity of wall materials, in: 7 Th Nordic Symposium on Building Physics, Reykjavik, 2005: pp. 662–669.

[31] D. Medjelekh, L. Ulmet, F. Gouny, F. Fouchal, B. Nait-ali, P. Maillard, F. Dubois, Characterization of the coupled hygrothermal behavior of unfired clay masonries: Numerical and experimental aspects, Building and Environment. 110 (2016). doi:10.1016/j.buildenv.2016.09.037.

[32] J. Kwiatkowski, M. Woloszyn, J.J. Roux, Modelling of hysteresis influence on mass transfer in building materials, Building and Environment. 44 (2009) 633–642. doi:10.1016/j.buildenv.2008.05.006.

[33] S. Roels, H. Janssen, A comparison of the Nordtest and Japanese test methods for the moisture buffering performance of building materials, Journal of Building Physics. 30 (2006) 137–161.